

comprehensive literature survey of the research carried out in Volt/VAR control, CVR implementation and assessments of its effect with and without the presence of DER. Finally, the chapter concludes with the research objective and detailed organization of the thesis.

## **Chapter 2: Concept of Smart Grid Enabled CVR**

In this chapter, a smart grid-enabled CVR methodology has been introduced. The basic concept of the proposed methodology has also been described. Further, the proposed methodology has been implemented using traditional LDC scheme with the help of conventional VVC devices such as OLTC, AVR and capacitor banks. Besides, the effect of different load models on CVR operation has been analyzed. In addition, assessment of the CVR effect with additional reactive power support from capacitor banks has also been carried out. Finally, the proposed methodology and its effects have been demonstrated on the modified IEEE 13-node and 34-node distribution feeder test system

## **Chapter 3: Distributed Energy Resources Impact on CVR**

This chapter describes the impact of DER on CVR energy savings and distribution grid operations. Besides, the combined effect of DER and CVR has also been analyzed using proposed smart grid-enabled CVR method. The PV smart inverter-based voltage and reactive power control of the ADN have been introduced in this chapter. In addition, the LDC approach has also been utilized to implement the proposed methodology. At last, the proposed smart PV inverter based VVC methodology has been validated on a modified IEEE 123-node unbalance distribution feeder test system. Moreover, the modeling and simulations have been carried out on OpenDSS and MATLAB platforms.

## **Chapter 4: Optimal CVR: Centralized Volt/VAR Optimization**

In chapter 4, the implementation of optimal CVR in ADN using VVO methodology has been introduced. A centralized discrete gravitation search algorithm-driven VVO

approach has been proposed in this chapter. Further, the proposed methodology has been validated in the presence of distributed energy storage and also analyzed the combined impact of both CVR and DES technology on peak load management and energy savings. In this chapter, the community energy storage type DES has been considered and correspondingly its power flow control scheme for an unbalanced power system has also been introduced. Finally, the proposed VVO based CVR methodology has been validated on a modified IEEE 123-node unbalance distribution feeder test system.

### **Chapter 5: Multi-Time Multi-Objective Volt/VAR Control and Optimization**

This chapter introduces a multi-time multi-objective VVC and optimization for CVR implementation. A multi-stage- multi-objective VVC methodology in a slow and fast time scale has been proposed in this chapter. In addition, for slow time scale operation, centralized VVO approach has been introduced and optimization problem has been solved using multi-objective particle swarm optimization. Further, a droop-based approach for fast time scale to control the PV DER reactive power has been introduced. In addition, the impact of cloud transients on PVs power production has also been analyzed. Besides, the economic impact of the proposed method has been described. Lastly, the proposed MSMO-VVC methodology has been validated on a modified IEEE 123-node unbalance distribution feeder test system.

### **Chapter 6: Time Horizon-based Model Predictive Volt/VAR Optimization in Presence of Electric Vehicle Charging Loads**

This chapter investigates on the need of coordinated operation of CVR in the presence of electric vehicle penetration in the active distribution network. A time horizon-based model predictive VVO methodology has been introduced in this chapter. The developed control algorithm considers the uncertainties in load demand and PV power generation. This chapter also describes the implementation of voltage and VAR regulation through

smart inverters of PVs and EV charging stations in global as well as local domains simultaneously. In addition, a real-time Volt/VAR droop-based controller has been introduced to control the smart inverter's reactive power dispatch. Finally, the proposed model predictive VVO algorithm has been tested and validated on a modified IEEE 34 bus test system.

### **Chapter 7: Real-Time Event-Driven Predictive Volt/VAR optimization and Control**

This chapter analyzes the impact of CVR in the presence of active devices such as solar photovoltaic (PV) and developed control algorithms in a real-time framework. An event-driven predictive framework for real-time VVO, along with a local two-level adaptive volt/VAR droop-based control algorithm for ADMS, is introduced in this chapter. Further, the proposed methodology has been validated in a real-time framework using the real-time digital simulator platform through co-simulation with models based on Python and OpenDSS.

### **Chapter 8: Conclusion & Future Work**

Finally, this chapter summarizes the research work. The significant contributions and conclusions of the present work are drawn in this chapter. In addition, this chapter also gives the future prospects of the present work.

#### **1.8. Conclusion**

This chapter briefly describes the overview of the distribution network, its classification and working principle of different VVC devices. In addition, the concept of smart Volt/VAR control and principle of CVR has been explained. This section also discussed the required literature review. Finally, chapter one concludes with the research objectives and outline of the present thesis.

**2.1 Introduction**

The basic aim of CVR technology is the conservation of energy by a marginal reduction in voltage (normally 2- 6% of nominal value) at user end nodes. Thus, by setting the regulation voltage in the ANSI lower half (114-120V) range, saving in energy can be achieved. However, while reducing the voltage, CVR should meet the International Standards ANSI C84.1–2006 [33]. Application of CVR with traditional schemes has not been found much effective because of restricted voltage reduction range, inaccurate load modeling and the unavailability of end-user information. In order to overcome the above barriers, enhance the observability of the distribution network and achieve higher energy savings, a smart grid-enabled CVR approach has been proposed in this chapter. The proposed CVR scheme has been implemented using closed-loop VVC methodology. The traditional LDC approach has been utilized in order to perform the VVC operation. The proposed methodology has been validated by analyzing the effect of different load models on CVR. Besides, the impact of additional reactive power compensation through CBs has been investigated during deeper voltage reduction range. The allocation of CBs has been done based on voltage sensitivity and fulfilling the objective of loss minimization.

**2.2 Smart Grid Enabled CVR**

The operation of CVR through a smart VVC approach is carried out by enabling of smart grid assets (such as ADMS, AMI and smart controllers) in local as well as the global domain of the distribution network. The schematic diagram of the integrated VVC with CVR for a distribution network has been shown in Figure 2.1.

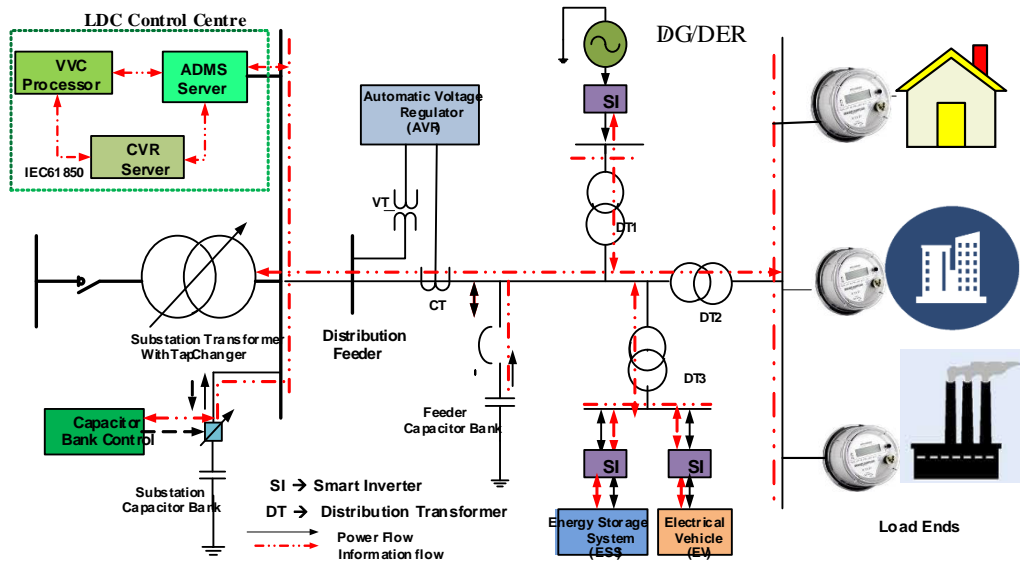


Figure 2.1. Proposed substation based Smart Grid-enabled CVR

In order to achieve the maximum energy savings, VVC processor calculates the controlled parameters of different field assets with the coordination of CVR server with ADMS. The field devices are connected to the servers through communication links. An ADMS regularly monitors and evaluates the power and voltage profile throughout the distribution network with the help of AMI and supervisory control and data acquisition (SCADA) systems. The proposed scheme first accumulates the measurements and then generates proper control signals. These control signals are transmitted through suitable communication links to VVC field devices. Accurate loads are derived through AMI data, which plays a prime role in enabling the CVR scheme in planning or in the real-time framework.

The assessment of CVR effects is judged through the CVR factor. Mathematically in terms of energy ( $CVR_{fE}$ ), it is calculated as the ratio of the total  $E_{Saving}$  in percentage and amount of voltage reduction ( $\Delta V$ ) over a time horizon in percentage as articulated in equations (2.1) and (2.2).

$$E_{Saving} = \left( \frac{E_{No-CVR} - E_{CVR}}{E_{No-CVR}} \right) \quad (2.1)$$

$$CVR_{fE} = \frac{(E_{saving})\%}{\Delta V\%} \quad (2.2)$$

## 2.3 Implementation of Proposed Methodology Using Traditional Approach

The proposed CVR scheme is implemented through controlling the voltage and reactive power flow in the network, which is governed by regulating the VVC devices such as OLTC/regulator and CB bank. The functional control schemes of these devices are described below subsection.

### 2.3.1 OLTC/Regulator Control

The traditional LDC scheme has been adopted in this investigation to control the OLTC/regulator. The control circuitry of AVR is governed by LDC to regulate the tap position of OLTC. Figure 2.2 shows the schematic diagram of the LDC model, which consists of a compensation circuit, voltage relay, and OLTC movement mechanism.

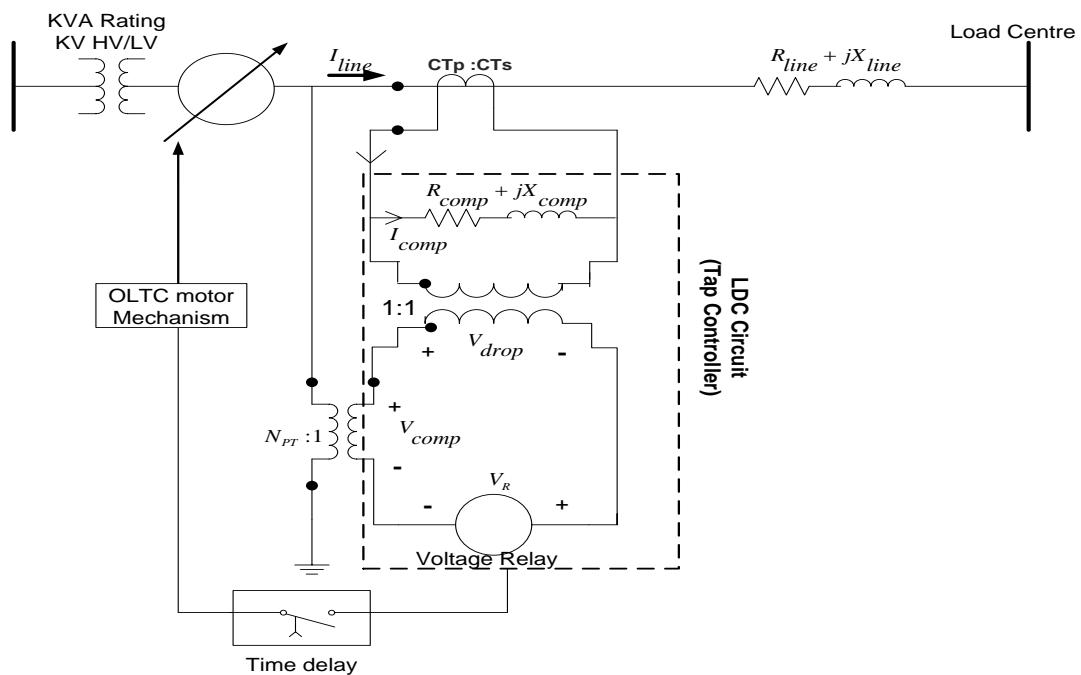


Figure 2.2 Schematics of LDC mechanism

The compensation circuit has a current transformer (CT), potential transformer (PT) and impedance matching transformer with R & X setting. These settings of compensation circuit are very critical for voltage regulation because it reveals when tap change is required. In this work, the R and X settings are referred as  $R_{comp}$ ,  $X_{comp}$  which represent the equivalent impedance from the regulator location to the regulation point. The detailed explanations regarding tap calculation can be found in [18], [52].

To calculate the required tap following steps are executed by LDC algorithms:

- Determine the  $R_{comp}$ ,  $X_{comp}$  value in ohm and volts using following equations (2.3) and (2.4) respectively.

$$R_{comp} + jX_{comp} = (R_{line} + jX_{line}) \cdot \frac{CT_p}{N_{PT} \cdot CT_s} \quad (2.3)$$

$$R_{comp} + jX_{comp} = (R_{line} + jX_{line}) \cdot \frac{CT_p}{N_{PT}} \quad (2.4)$$

where,  $R_{line}$ ,  $X_{line}$  are the resistance & reactance of the line respectively and  $N_{PT}$  is PT ratio determined by equation (2.5).

$$N_{PT} = \frac{V_{LN, rated}}{V_{Base}} \quad (2.5)$$

- Calculate the actual (feeder) line current ( $I_{line}$ ) with the help of equation (2.6).

$$I_{line} = \left( \frac{KVA_{rated}^{Trf}}{\sqrt{3} KV_{rated}^{Trf}} \right) \quad (2.6)$$

- Find the compensator current ( $I_{comp}$ ) through equation (2.7).

$$I_{comp} = \left( \frac{I_{line}}{CT_{ratio}} \right) \quad (2.7)$$

- Compute input voltage to the compensator circuit or compensator voltage ( $V_{comp}$ ) by equation (2.8).

$$V_{comp} = \left( \frac{V_{LN}}{N_{PT}} \right) \quad (2.8)$$

Voltage drop ( $V_{drop}$ ) in compensation circuit is determined through equation (2.9).

$$V_{drop} = (R_{comp} + jX_{comp}) \times I_{comp} \quad (2.9)$$

- Calculate the voltage across the voltage relay ( $V_R$ ) using equation (2.10) which represents the voltage at regulation point.

$$V_R = V_{comp} - V_{drop} \quad (2.10)$$

- If  $V_R$  is outside the bandwidth of regulator then required tap change is calculated by equation (2.11). Otherwise, there is no need to change the tap position.

$$\text{Tap} = \frac{(V_{reg} \pm 1 - V_R)}{(\Delta V_r \times V_{base})} \quad (2.11)$$

$V_{reg}$  is regulation voltage at regulating position (set point), where,  $[V_{reg} \pm 1]$  is the acceptable range of  $V_{reg}$  of the distribution feeder.

- After calculating tap value, voltage relay sends the signal to the OLTC motor mechanism to change the tap position.

### 2.3.2 Capacitor Bank Control

CB control is very helpful to maintain the feeder voltage profile and reduce the system losses. This controller is supplemented with monitoring devices such as CTs, PTs and local decision processors with connector/discounter situated at the load side of the bus as shown in Figure 2.3. The controller device takes samples of voltage and current through CTs and PTs at the monitored location. After that, a decision is taken regarding the amount of compensation required based on control criteria such as kVAR and voltage at monitored points/devices.



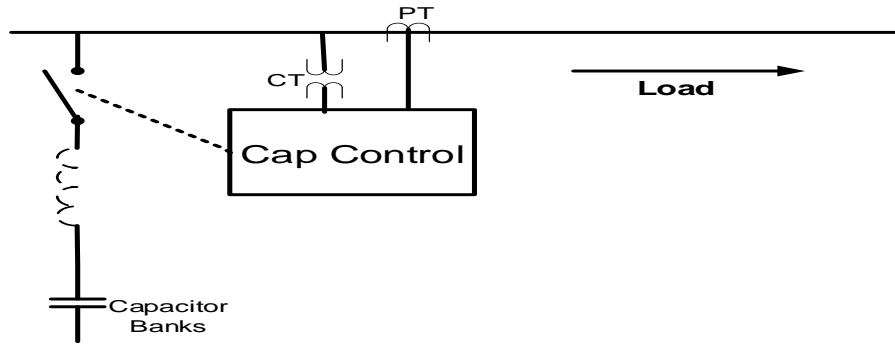


Figure 2.3 Capacitor bank controller with monitored devices

To control the voltage profile and reactive power flow at monitored point/device, the following *algorithm 1* are adopted to CB control as delineated under:

---

**If**  $V_{i,T}^{mon} < V_{i,T}^{\min}$   
     *CB module is switched ON,*

**else if,**  $V_{i,T}^{mon} > V_{i,T}^{\max}$   
     *CB module is switched OFF.*

**else if,**  $V_{i,T}^{\min} \leq V_{i,T}^{mon} \leq V_{i,T}^{\max}$   
     *check the Q limits*  
     **if,**  $Q_{i,T}^{mon} < Q_{i,T}^{\min}$   
         *CB module is switched ON,*  
     **else,**  $Q_{i,T}^{mon} > Q_{i,T}^{\max}$   
         *CB module is switched OFF.*

**end**  
**end**

---

The specified value of  $Q_{i,T}^{\min}$  is 40% of the rating of CBs and  $Q_{i,T}^{\max}$  is 60% of the rating of CBs in reverse direction.

### 2.3.3 Power Flow Algorithm

Conventional load flow methods such as Gauss-Seidel and Newton-Raphson are not suitable for distribution network because of most of the distribution feeders are radial with unbalanced loading pattern and untransposed lines. Due to fast convergence, the

iterative ladder technique is widely used in the radial distribution network. Ladder iterative algorithm uses forward/backward sweeping technique [18]. To determine the corresponding voltage and current backward sweep is applied to equations (1.1) and (1.5) while the forward sweep uses equation (1.4) to find the voltages in a distribution feeder. The sweeping process is repeated until the difference between the defined and the calculated source voltage is below the predefined tolerance limit [113].

## **2.4 Assessment of CVR Effect Under Different Load Models**

This section discussed the analysis of the CVR effect with different load models. The effect of CVR on energy consumption can be described by Joule's law, the power  $P$ , voltage  $V$  and current  $I$  in a resistive circuit satisfying  $P = VI$  with the assumption that there is no need of reactive power for consumer's devices. Lowering the voltage level reduces the power when the load consists of pure resistors with constant resistance  $R$ , followed by the ohm's law  $V = IR$  and  $P = V^2/R$ . From various CVR tests, it is observed that the CVR effect is highly influenced by the consumer's load type. In this work following types of load models have been used to analyze the CVR effect.

- Constant PQ Model
- Constant Impedance ( $Z$ ) Model
- Constant Current ( $I$ ) Model
- Constant ZIP Model
- Nominal Linear P, Quadratic Q Model

### *2.4.1 Case Study*

#### *VVC mode of operation*

- *Non CVR mode:* In this mode, effect of both AVR and CBs are considered in power flow analysis. The settings of regulators and CBs are the same, as mentioned in [114]. AVR1 and AVR2 have secondary voltage level 122V, 124V respectively.

- *CVR mode*: This mode includes the effect of both voltage regulators and CBs in power flow analysis. The voltage level of regulators has been reduced, and their modified values are 120V, 120V respectively.

#### 2.4.2 Test System and Description

For analysis of CVR effect IEEE 34-bus, 24.9 kV distribution feeder model has been considered in this study. The distribution model consists of 34 nodes, two voltage regulators, capacitor banks and different load models [114]. Modelling and power flow analysis of the distribution system has been carried out in OpenDSS platform developed by EPRI [113]. A similar load type has been considered at each node of the distribution feeder bus to analysis the CVR effect with the individual load model.

#### 2.4.3 Simulations and Result Discussion

This section presents CVR test simulation results with different load models. Power flow simulations have been done in *SNAP* mode with *STATIC* control mode in OpenDSS. The VVC operation has been carried out at peak demand hour with maximum loading condition (i.e.1 p.u). Various simulation results are analyzed below:

##### 2.4.3.1 Constant PQ Load:

This type of load model increases the energy consumption with the reduction of voltage level because of an increase in line losses due to more current is drawn by the loads. Constant PQ load is defined as *model 1* or constant P+jQ load in OpenDSS platform. Assuming all loads connected in the test system are constant PQ type. From Figure 2.4 and Figure 2.5, it can be seen that power demand and losses are increased in CVR mode in compare to non CVR mode. Hence, CVR operation is not beneficial for constant power load models.

#### 2.4.3.2 Constant Impedance (Z) Load:

Assuming all loads connected in the test system are constant impedance load type. Simulations have been carried out with both with constant Z load for both the mode of operation. From simulation results, as can be seen from Figure 2.4 and Figure 2.5, it is observed that there is a reduction in power demand and losses with CVR mode operation. Significant energy savings can be achieved with CVR mode operation.

#### 2.4.3.3 Constant Current (I) Load Model:

Assuming all loads connected in the considered test system are the constant current load type. Simulation results with Constant I load have shown in Figure 2.4 and Figure 2.5, and it is observed that energy saving is slightly improved with CVR mode. The reduction of energy consumption is less than in comparison to the constant Z load model.

#### 2.4.3.4 Constant ZIP Load Model:

Assuming all loads connected in the test system is a combination of constant impedance (Z), constant current (I) & constant power (P), or constant ZIP load type. The equations of the ZIP load have been shown in (1.17) - (1.20). Figure 2.4 and Figure 2.5 also shows the simulation results with constant ZIP load. From simulation results, it is observed that real power demand is reduced with the CVR effect. There is a slight reduction in real power losses has also been reported. Thus, it is observed that saving achieved in CVR mode in the presence of ZIP type load model is highly depends upon its coefficients. Moreover, ZIP coefficients represent the part of each load type. Generally, savings are influenced by the dominant value of the ZIP coefficient.

#### 2.4.3.5 Nominal Linear P, Quadratic Q Load:

Nominal Linear P, Quadratic Q Load, is defined as model 4 in the OpenDSS platform. The representation of this model looks like exponential type loads. Instead of exponents, this model usages the  $CVR_{f(kW)}$  and  $CVR_{f(kVAR)}$  as shown in equations (1.21-1.22)

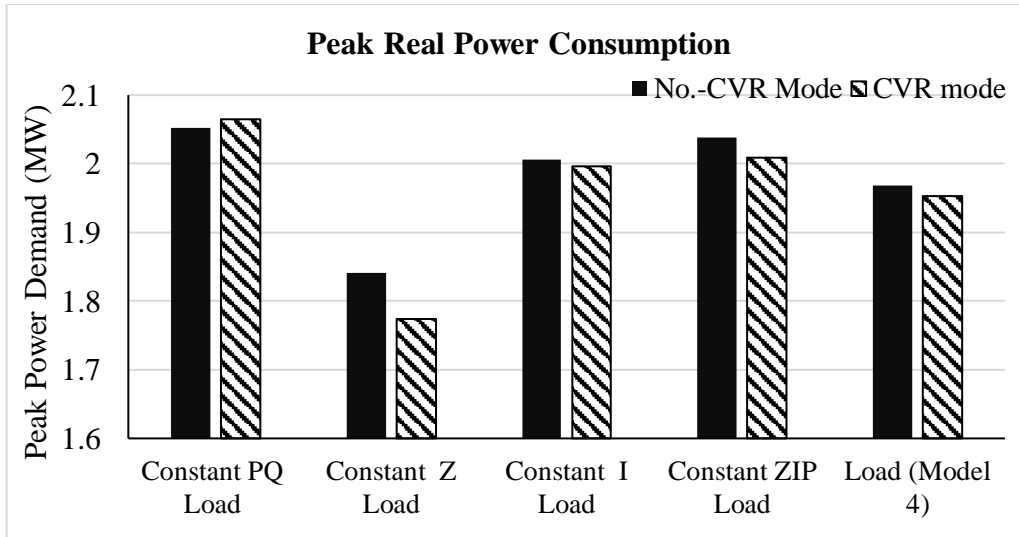


Figure 2.4 Peak real power consumption with and without CVR for different loads

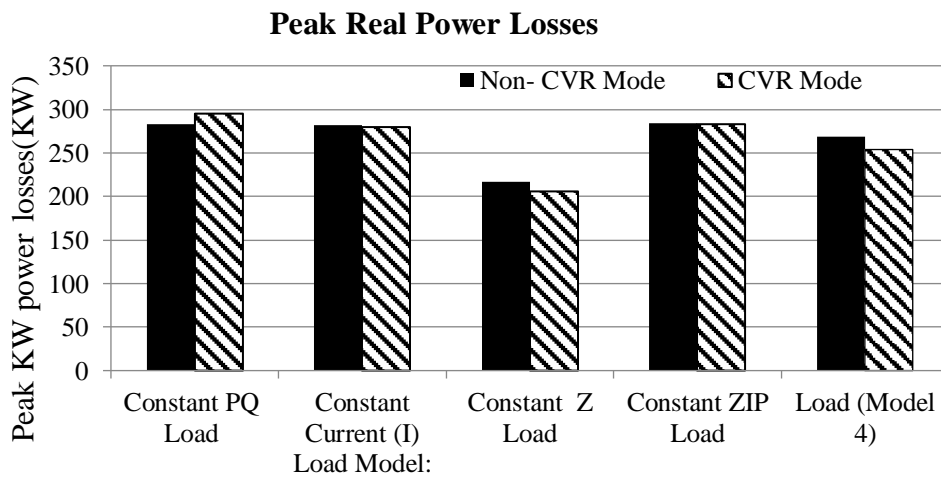


Figure 2.5 Peak real power losses with and without CVR for different load models

respectively. In this study, the simulations with model 4, the value of  $CVR_{f(kW)}$  and  $CVR_{f(kVAR)}$  is 0.8 and 2.0 is considered respectively. From results, it can be observed that operating in CVR mode, power demand and power losses reduced in comparison to non-CVR mode operation. Considerable energy savings can be achieved with CVR operation.

From the analysis of all simulation results, it can be concluded that a significant amount of energy savings can be obtained with CVR operation. The impact of different load models highly influences the CVR operation, and violation of voltage limits is also a matter of concern.

#### *2.4.4 Observation and key findings*

- The proposed smart grid-enabled CVR algorithm is more beneficial in comparison to traditional CVR.
- The highest energy savings can be achieved with constant impedance (Z) loading in the contest to other load models.
- Generally, loads are mixed types such as ZIP model; in such cases, a considerable energy saving can also be achieved.
- While applying CVR schemes, system losses may increase or decrease.
- CVR operation shows the adverse effect during the presence of constant power loads
- During deeper voltage reduction, voltage violation cases may occur in some parts of the distribution network.

Therefore, an additional reactive power source is required to lower the losses and maintain the voltage profile throughout the feeder end.

## **2.5 Assessment of CVR effect with additional Reactive Power Support**

The effect of end-users loading patterns in CVR operation plays a crucial role. Thus, an accurate load model is required to check the effectiveness of CVR operation. Moreover, during the execution of CVR under a deeper voltage reduction range, voltage violations may occur in some parts of the distribution network or near to load to voltage-sensitive nodes. In this context, the CVR study has been carried out with different voltage reduction levels considering the voltage dependent load models. Besides, additional reactive power support has been injected through optimally placed capacitor banks during the deeper voltage reduction to maintain voltage profile within limits.

### *2.5.1 Methodology*

In order to maximize the energy savings and peak demand reduction, VVC operation is carried out with CVR. The VVC problem has been formulated in two parts; the first is the implementation of Voltage and VAR controllers and second is an optimal allocation of reactive power support devices for loss minimization during the CVR operation. The modeling of voltage control devices such as AVR/OLTC and CBs have already discussed in the previous *chapter 1 in section 1.4*.

#### *2.5.1.1 Volt/VAR Controllers*

In CVR operation, regulator controllers of AVR are used known as reg control and capacitor banks are controlled through cap control. These controllers are inbuilt in OpenDSS. Figure 2.6 demonstrates the CVR operation using the VVC algorithm.

#### *2.5.1.2 Power Loss Minimization*

The distribution network has high power losses in comparison to another part of the power system. As consequences of large distribution power losses raise the peak power demand, poor voltage profile and generation cost. Therefore, the loss minimization problem is very crucial for the optimal operation of the distribution feeder.

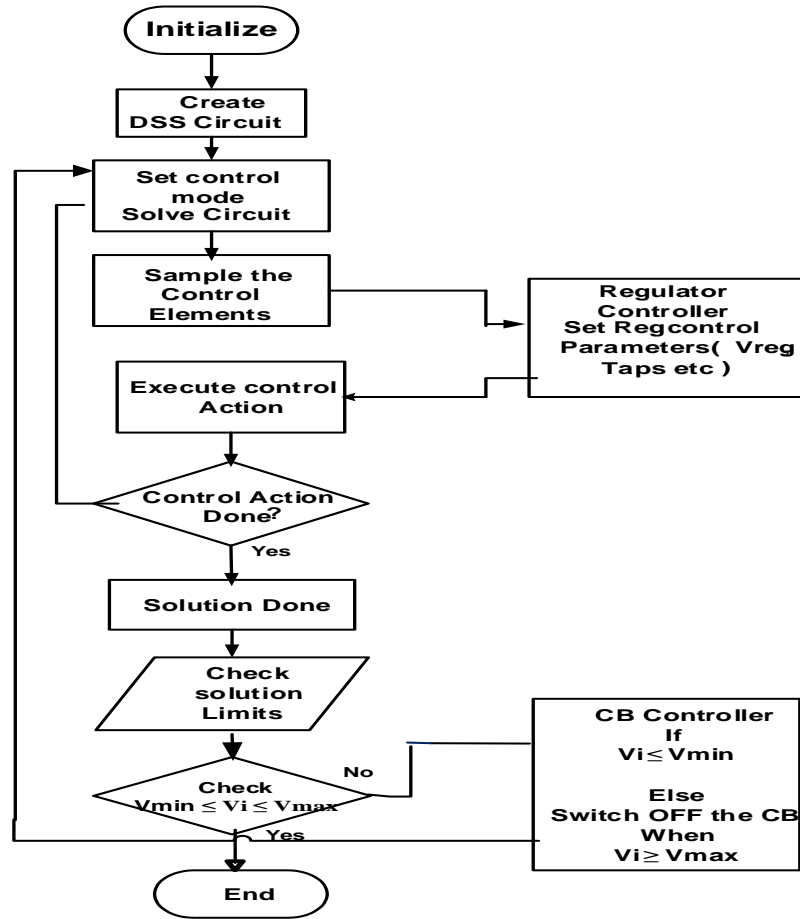


Figure 2.6 Flowchart of VVC operation for CVR mode

The optimization problem in distribution network look like something as shown in the below equation (2.12) [88]

$$\min_{\underline{y}} f(\underline{x}, \underline{y}) = P_{Loss} \quad (2.12)$$

$$s.t. \quad \underline{g}(\underline{x}, \underline{y}) = 0 \quad (2.13)$$

$$V_{min} \leq V_i \leq V_{max} \quad (2.14)$$

Where  $\underline{g}(\underline{x}, \underline{y}) = 0$  is the distribution power flow equation.  $V_i$  is the voltage at the  $i$ th bus.

In order to minimize the system losses, the equation (2.12) find out the required reactive power injection support per node while satisfying the voltage its tolerance limit. Many optimization techniques are available to solve the problem discussed in the above equation (2.12).



In this work, a search technique inbuilt in OpenDSS has been utilized for optimal placement of CBs to find the optimal solutions. Moreover, OpenDSS has an internal Autoadd mode for the minimization of losses. OpenDSS uses ladder iterative method to determine the unknown voltages and currents. So Autoadd mode takes advantage of direct access to the compensation current array in the solution [28], [113]. In order to move a capacitor from node to node, it only needs alternation in the compensation current array. In this technique, solution convergence speed also increased because the admittance matrix remains unchanged and there is no need to re-factorized the admittance matrix. Generally, it takes 2-4 iterations in every solution and produces outputs in percentage per node. Percentage improvement shows the next best location to supply reactive power. Figure 2.7 shows Autoadd optimization technique for loss minimization.

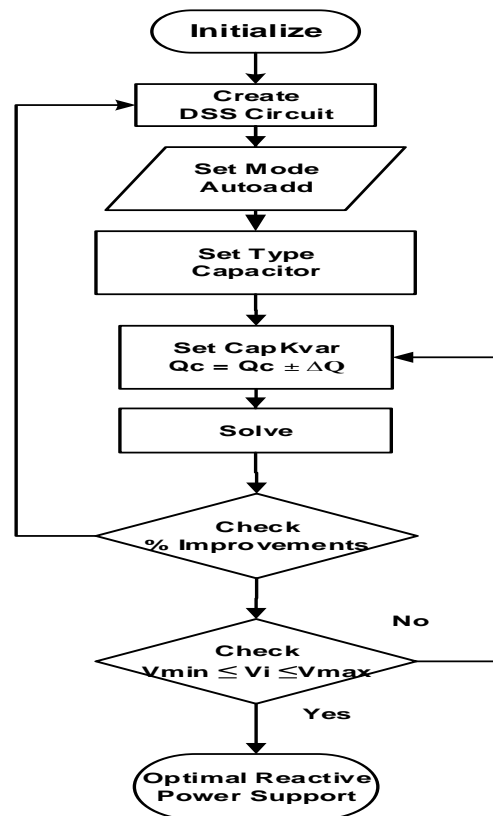


Figure 2.7. Flow chart for optimization Using Autoadd

## 2.5.2 Simulations and Result Discussion

### 2.5.2.1 Test System and Descriptions

For assessment of CVR effect, an IEEE, 13 node distribution test feeder with voltage-dependent loads has been considered. The distribution model consists of 13 nodes, one voltage regulators, two capacitor banks and different load models [114]. Modeling and power flow analysis of the distribution system has been carried out in OpenDSS platform developed by EPRI [113]. Before performing simulation of the test system some assumptions are considered such as (i) DMS and communication system is working well and its delay effect not considered during the execution of CVR operation (ii) Same load models are considered throughout the distribution network with and without CVR operation considering load allocation factor 1 in OpenDSS inbuilt load allocation algorithm. (iii) Effect is neglect during the operation of switched shunt capacitor banks.

### 2.5.2.2 VVC modes of operation

Test feeder has been simulated in three different modes considering constant ZIP and Nominal Linear P, Quadratic Q (feeder mix) type load models (the detail explanation can be seen *chapter 1* under subsection *1.4.2.4*) with different voltage reduction (VR) level as discussed under:

- *No- CVR Mode:* IEEE 13 node test system is simulated with VVC devices in normal operation with a regulated voltage of 125V with no voltage reduction.
- *Base CVR Mode:* In this mode, IEEE 13 node test system is simulated with VVC devices in CVR operation through LDC setting with the regulated voltage at 122V, 119V, 118 V, or reduction of the voltage level at 2.4%, 4.8%, and 5.6% respectively. No additional reactive power injected to minimize the system losses.
- *CVR with Reactive Power Support (RPS) Mode:* In this mode, additional reactive power support is provided during the deeper CVR operation to minimize the losses and

maintain the feeder voltage limits. Capacitor banks are used here as an additional reactive power support source.

### 2.5.2.3 Case Study

- *Case-I. Effect of Constant ZIP Load model:* Analysis of voltage reduction with voltage-dependent constant ZIP type load model has been discussed in this case. ZIP coefficients used in this model are the mixture of residential, commercial and industrial type loading areas taken from [53]. From Table 2.1, it can be seen that during the base-CVR mode, about 1.12 to 2.33% peak MW load demand reduction is achieved. However, peak kW losses are also increased (0.06 to 0.17%) slightly because of the incremental rise in current in conductors. This small increase in losses is not so effective with the comparison of achieved peak load relief. However, there is a voltage violation case (crosses the minimum voltage limit of 0.95 p.u) that has been observed with the higher voltage reductions (4.8%, 5.6%) during the base-CVR mode.

**Table 2.1** Analysis of CVR effect with ZIP (mix) load

<b>Terms</b>	<b>No-CVR</b>	<b>Base-CVR</b>			<b>CVR with RPS</b>	
<b>Voltage Reduction (%)</b>	0.0	2.4	4.8	5.6	4.8	5.6
<b>Minimum Voltage (p.u)</b>	0.9882	0.9619	0.9373	0.9353	0.9534	0.953
<b>Peak MW Demand</b>	3.6146	3.5741	3.5389	3.5301	3.5376	3.524
<b><math>\Delta P_{\text{demand}}</math> kW, (%)</b>	---	- 40.5 (-1.12)	-75.7 (-2.09)	-84.50 (-2.33)	-77.0 (-2.13)	-88.6 (-2.45)
<b>Peak kW Losses, (%)</b>	109.83 (3.03)	111.87 (3.09)	114.86 (3.17)	115.87 (3.2)	104.16 (2.89)	104.0 (2.88)
<b><math>\Delta P_{\text{losses}}</math> in kW, (%)</b>	--	+2.04 (+0.06)	+5.03 (+0.14)	+6.04 (+0.17)	-5.67 (-0.14)	-5.83 (-0.21)

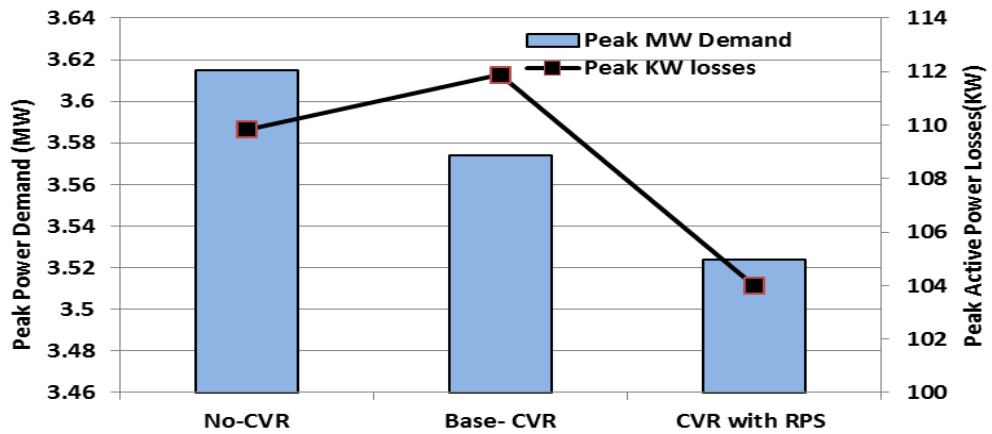


Figure 2.8 Peak demand & peak losses with ZIP load model

This issue has been resolved through CVR with RPS mode. In this mode, the additional, RPS is provided though optimally placed CBs of 100 kVAR and 120 kVAR at each phase of the nodes 611,671,684 for 4.8%, 5.6% of voltage reduction respectively. About 2.45% power demand and 0.21% loss reduction is reported with the operation of CVR with RPS mode. Figure 2.8 clearly shows that peak demand and losses are decreasing during the CVR with RPS mode with improved voltage profile.

- *Case-II Nominal Linear P, Quadratic Q (feeder mix) load:* This feeder mix load model, also known as model 4 in OpenDSS. In model 4 value of CVRwatts and CVR vars are 0.8, 2 considered respectively. Table 2.2 shows the simulation results with the different modes of operation of CVR with different VR levels. In base CVR mode, there is about 1.82 to 4.06 % peak MW load demand reduction is achieved. However, peak load kW losses are also increased slightly with voltage limits violations during the higher voltage reduction level as 5.6%. In order to satisfy voltage limits, simulation is carried out in CVR with RPS mode with the addition of capacitor banks of 100 kVAR at each phase of 611,671, 684 nodes. Figure 2.9 shows the peak demand & peak Losses during CVR operation. From simulation results, it has been observed that both demand (4.3%) and losses (0.2%) are reducing though the enabling of CVR with RPS mode.

A comparative CVR effect with ZIP load model and model 4 have been shown in Figure 2.10 and also observed that power demand is decreasing more in model 4 as compare to ZIP load model with different voltage reduction level.

**Table 2.2** Analysis of CVR effects with Model 4

Terms (V&P)	No CVR	Base-CVR			CVR with RPS
VR(%)	0.0	2.4	4.8	5.6	5.6
Min. Volt. (p.u)	0.9936	0.96912	0.9504	0.9348	0.95189
Peak MW Demand	3.6262	3.5603	3.5238	3.4789	3.4727
$\Delta P_{\text{demand}}$ kW (%)	---	-65.9 (-1.81)	-102.4 (-2.823)	-147.3 (-4.06)	-153.6 (-4.3)
Peak kW Losses, (%)	107.41 (2.962)	107.65 (2.968)	107.82 (2.97)	109.69 (3.02)	100.04 (2.76)
$\Delta P_{\text{losses}}$ in kW (%)	--	+0.14 (+0.004	+0.41 (+0.008	+2.82 (+0.038	-6.37 (-0.2)

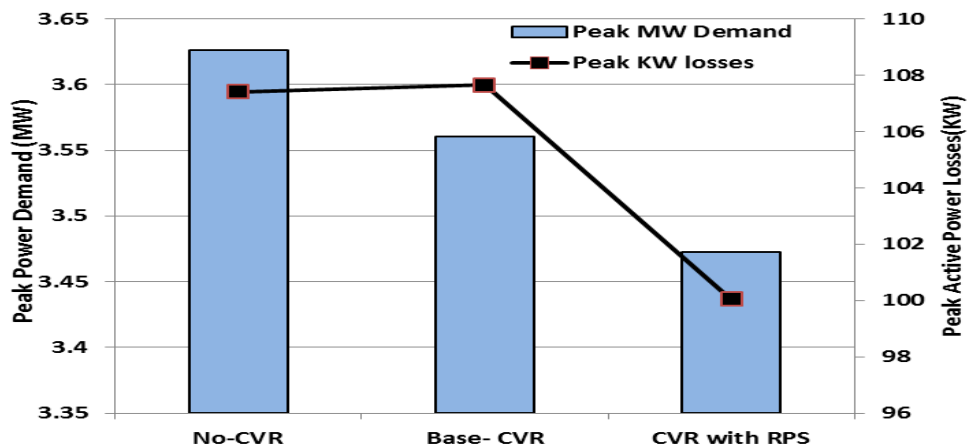


Figure 2.9 Peak demand and peak losses with load model 4

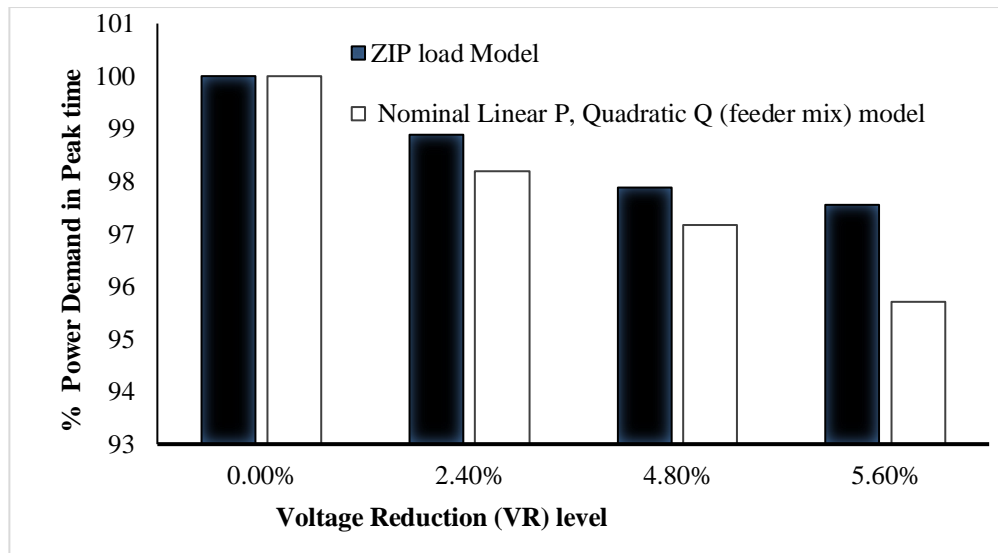


Figure 2.10 Percentage load demand in peak during CVR operation

### 2.5.3 Important Observations and Findings

- A significant amount of peak load relief is achieved
- CVR is more effective with reactive power support for a higher level of voltage reduction.
- The reactive power support through other sources such as distributed energy resources, distributed energy storage and electric vehicles is also needed to analyze

## 2.6 Conclusion

This chapter proposed a closed-loop smart grid-enabled CVR methodology for energy conservation in the distribution network. The proposed methodology has been validated under two scenarios (i) analyzing the impact of different load models on CVR and achieved energy savings in power distribution system and (ii) the impact of additional reactive power support through CBs under CVR operations. The effect of loading pattern during CVR operation also carried out, and it is analyzed that the accurate load model and loading pattern also affect the CVR savings. From simulation results, it is observed that a significant amount of peak load relief is achieved with minimum losses. CVR operation

with reactive power support is more effective for reducing the demand for system losses in comparison to without reactive power support. To achieve more savings and demand reduction smart grid-enabled CVR scheme is more beneficial in comparison to tradition CVR. Though reactive power support through capacitor banks is not so much effective solution, but for peak demand and loss reduction, it may be used where constraint cost is not a big issue.

For better controlling and coordination, CVR has to combine with DERs, and smart inverter has to participate in voltage regulation as recommended by the new IEEE 1547 - 2018 standard. In this context, the combined effect of CVR and DERs will be analyzed in the next *chapter 3* including the impact of the smart inverter as a voltage control device.